

RESEARCH ARTICLE

 OPEN ACCESS

Effect of SOF/VEL Antiviral Therapy for HCV Treatment: A Control Theoretic Approach

Jayanta Mondal^a, Piu Samui^a, Amar Nath Chatterjee^b^aDepartment of Mathematics, Diamond Harbour Women's University, Sarisha, West Bengal-743368, India; ^bDepartment of Mathematics, K. L. S. College, Nawada, Magadh University, Bodh Gaya, Bihar-805110, India**ABSTRACT**

Liver cirrhosis and hepatocellular carcinoma diseases are caused by Hepatitis C virus (HCV) infection. Inside this article, a deterministic model is proposed and analysed for the transmission of HCV infection in the liver cells considering two types of viral strain (wild and mutant). We also projected a mathematical model to study the effects of Sofosbuvir (SOF) together with Velpatasvir (VEL) antiviral therapy in HCV infected patients. Our analytical as well as numerical findings assist to detect the optimal strategy of treatment depending on the circumstances in controlling the HCV infection.

ARTICLE HISTORYReceived November 26, 2020
Accepted August 21, 2021**KEYWORDS**HCV, SOF/VEL,
Optimal control problem,
Sensitivity analysis,
Efficiency analysis,
Cost-effectiveness

1 Introduction

Worldwide more than seventy million people are suffering from chronic Hepatitis C virus (HCV) infection ([World Health Organization, 2020](#)). In 2016, WHO declared that approximately 399,000 people died due to Hepatitis C virus infection (pre-dominant causes are liver cirrhosis and hepatocellular carcinoma).

Formerly in 1998, [Neumann et al.](#) studied the dynamical behaviors of the HCV infection, and thereafter its changes when Interferon- α therapy is prescribed to reduce the production of virions. Later [Dahari et al. \(2007\)](#) extended the model proposed by Neumann et al. by incorporating the term “proliferation of hepatocytes” (hepatocytes are the chief parenchymal cells of the liver), and the model proves the existence of “critical drug control” along with an explanation regarding “biphasic” and “triphasic” decline of virions. In 2004, [Dixit et al.](#) showed how in antiviral treatment of HCV infection, Interferon response might be improved by Ribavirin. [Chatterjee et al. \(2019\)](#) studied the discrete role of Cytotoxic T Lymphocytes (CTL) during the HCV infection. [Chatterjee and Kumar \(2020\)](#) also studied the effect of CTL boosting through vaccination during the Hepatitis C virus infection. Also, the mechanism of combined therapy using Interferon and Ribavirin is investigated through various mathematical models ([Powers et al., 2003](#); [Feld and Hoofnagle, 2005](#); [Banerjee et al., 2013](#)). [Chakrabarty and Joshi \(2009\)](#) proposed a mathematical model to capture the effects of optimal control using two drugs, Interferon and Ribavirin in minimizing the viral load and controlling the side effects of the used drugs.

In HCV treatment management, direct-acting antivirals (DAA) have a pivotal role to HCV infected patients with high rates of antiviral response. DAA also improve the tolerability and reduce the treatment period ([Chatterjee et al., 2021](#)). Sofosbuvir (SOF) and Velpatasvir (VEL) are DAA agents acting against HCV with pan-genotypic activities and a high barrier of resistance ([Von Felden et al., 2018](#)). Sofosbuvir is a nucleotide analog of HCV polymerase inhibitor which means that it blocks the polymerase enzyme essentially used by the virus to reproduce. It specifically inhibits HCV NSSB (nonstructural protein 5B) RNA-dependent RNA polymerase ([Mogalian et al., 2017](#)). Velpatasvir prevents viral replication by inhibiting nonstructural protein 5A (NS5A), a non-enzymatic viral protein that plays a key role in HCV replications assembly, and modulation of host immune responses ([Mogalian et al., 2017](#)).

The SOF/VEL is a combination of two pan-genotypes, with high potency and high barrier antiviral molecules which provides more than 95% of sustained virologic response (SVR) ([Von Felden et al., 2018](#)). Notably, Velpatasvir has a significant higher barrier in resistance than the first generation NS5A inhibitors ([Lawitz et al., 2016](#)). The SOF/VEL combination is used alone or with Ribavirin (Copegus, Rebetol, Ribasphere) to treat chronic Hepatitis C patients. The single-pill of SOF/VEL combination once-a-day improves the adherence to the therapy. It is also observed that administration of SOF/VEL produces a significant

improvement in patients' quality of life (Younossi et al., 2016, 2017, 2016). Patients reported outcomes are revealed from the SOF/VEL registered trials obtained in more than 1800 HCV chronically infected subjects (Von Felden et al., 2018).

Our proposed model deals with the dynamic behaviors of the Hepatitis C virus infection. We have extended the model by including an optimal control of HCV infection using a combination of drugs (SOF/VEL) that reduces the cellular infection rate inhibiting viral replication. For a combined drug therapy, sometimes harmful side effects, as well as the ineffectiveness of treatment after a certain time, occur due to mutation of the virus and it causes the resistance to the treatment. The optimal control technique is applied with SOF/VEL combined therapy to observe appropriate treatment strategies which will yield a decline in viral reproduction and lessen the side effects of the therapy. Here the treatment persists for a given period of time initiating from t_0 to final time t_f . However, the results are not interval-dependent. In this paper, we specifically deal with optimizing treatment scheduling i.e when and how the treatment should be introduced.

The mathematical tools, consequent analytic results, and numerical findings are coordinated in the following order for better understandings of the HCV infection: In the very next Section 2, we present an aggregate formulation of the proposed mathematical model of Hepatitis C virus infection. Section 3 is accompanied by some basic properties of the model such as positivity and boundedness of the solutions of the system, the existence of an infection-free steady state and an endemic steady state, and the basic reproduction number (\mathcal{R}_0) of the system. Section 4 is showing an outline about the local stability of the steady states and occurrence of transcritical bifurcation at the infection-free steady state and the global stability of the endemic steady state choosing an appropriate Lyapunov function is shown in Section 5. The sensitivity analysis of the baseline parameters corresponding to \mathcal{R}_0 is chalked out in Section 6. Next, an optimal control problem through an objective functional with two controls is discussed in Section 7. To confirm the gained analytical results aligned with the biological process of HCV infection, Section 8 is designed with numerical simulation. A discussion (in Section 9) regarding the results obtained from the previous sections is drawn and we convey conclusions to support the overall findings.

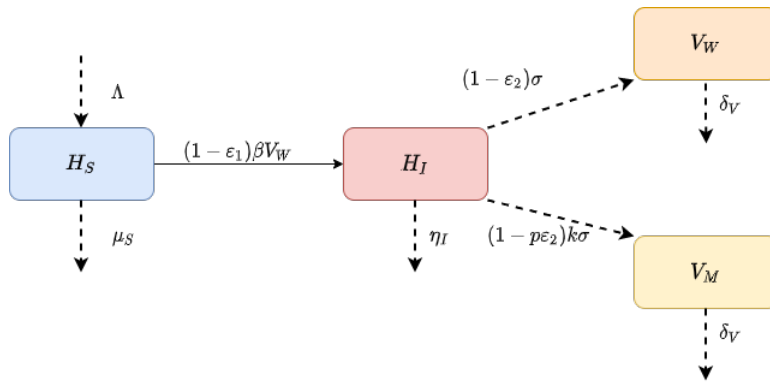


Figure 1: The schematic flow diagram of the model (1) represents the dynamics of Hepatitis C virus infection for the healthy liver cells (H_S), infected liver cells (H_I), wild Hepatitis C virus (V_W), and mutant Hepatitis C virus (V_M).

2 Structure of the Compartmental Model

In this research article, we study the noteworthy effects concerning the replication of Hepatitis C virus where the replication process of HCV happens mainly in the liver cells. Here we consider four variables: healthy (uninfected) liver cells (H_S), infected liver cells (H_I), and two strains of the virus: wild virus strain (V_W) and mutant virus strain (V_M). Wild-type or drug sensitive strain mainly dominates the infection at initial stage. On the other hand, the mutant or drug-resistant strain has no infectivity. Then the model is

$$\begin{aligned}
 \frac{dH_S}{dt} &= \Lambda - (1 - \varepsilon_1)\beta H_S V_W - \mu_S H_S, \\
 \frac{dH_I}{dt} &= (1 - \varepsilon_1)\beta H_S V_W - \eta_I H_I, \\
 \frac{dV_W}{dt} &= (1 - \varepsilon_2)\sigma H_I - \delta_V V_W, \\
 \frac{dV_M}{dt} &= (1 - p\varepsilon_2)k\sigma H_I - \delta_V V_M,
 \end{aligned} \tag{1}$$

with non-negative initial condition

$$H_S(0) = \theta_1, \quad H_I(0) = \theta_2, \quad V_W(0) = \theta_3, \quad V_M(0) = \theta_4. \quad (2)$$

Here we assume that the healthy liver cells are produced at a constant rate Λ and μ_S indicates their death rate. Disease transmission rate β indicates the rate at which healthy liver cells become infected and η_I is the death rate of infected liver cells. Wild type or mutant type virus are generated at the rate σ or $k\sigma$, respectively, where $k \in (0, 1)$ is the relative capability of the mutant strain in relations of viral replication. It is assumed that δ_V is the removal or clearance rate of both wild type and mutant type virus from plasma. The control input of SOF doses is ε_1 and ε_2 stands for control input of VEL doses. Thus the wild type viral production is decreased by a factor $(1 - \varepsilon_2)$. The mutation rate of Hepatitis C virus is diminished with a factor $p \in [0, 1)$ and thus the mutant virus production be reduced at a rate $(1 - p\varepsilon_2)$. Here all model parameters are non-negative. Also the drug controls of SOF and VEL satisfy the relation $0 \leq \varepsilon_1, \varepsilon_2 < 1$. The dynamical structure of the system is explained through the Figure 1.

Table 1: Set of biologically relevant parameter values used for numerical simulation.

Parameter	Biological Meaning	Assigned value (unit)	Source
Λ	Constant production rate of healthy liver cells	10 cell ml ⁻¹ day ⁻¹	Wodarz, 2005
ε_1	Control of SOF	$0 \leq \varepsilon_1 < 1$	
β	Rate of infection / transmission	0.01 ml day ⁻¹ cell ⁻¹	Wodarz, 2005
μ_S	Natural death rate of healthy liver cells	0.04 day ⁻¹	fit for model
η_I	Natural death rate of infected liver cells	1.0 day ⁻¹	Dahari et al., 2009
ε_2	Control of VEL	$0 \leq \varepsilon_2 < 1$	
σ	Virions production rate	2.9 virions cell ⁻¹ day ⁻¹	Dahari et al., 2009
δ_V	Removal rate of both wild and mutant strain	2.4 day ⁻¹	Smith and De Leenheer, 2003
p	Mutant strain reducing factor	$0 \leq p < 1$	
k	Relative fitness of mutant strain	$0 < k < 1$	

3 General Structural Properties of the System

Theorem 1. *Let the non-negative initial condition (2) be satisfied for the system (1), then a positive invariant set*

$$\Omega = \left\{ (H_S, H_I, V_W, V_M) \in \mathbb{R}_+^4 : H_S + H_I \leq \frac{\Lambda}{\mu_S}, V_W + V_M \leq \varpi_V \right\},$$

where $\varpi_V = \min \left\{ \frac{(1-\varepsilon_2)\Lambda\sigma}{\delta_V\mu_S}, \frac{(1-p\varepsilon_2)k\sigma\Lambda}{\delta_V\mu_S} \right\}$ exists if all the solutions (H_S, H_I, V_W, V_M) of the system (1) are non-negative and finite upper limit of Ω exists.

Proof. First we show that all the four state variables of the system (1) satisfying the initial condition (2) are non-negative. From the first equation of system (1), we can write

$$\begin{aligned} \frac{dH_S}{dt} &= \Lambda - (1 - \varepsilon_1)\beta H_S V_W - \mu_S H_S \\ &= \Lambda - \zeta H_S, \end{aligned}$$

where, $\zeta = (1 - \varepsilon_1)\beta V_W + \mu_S$. Then on integration, we get

$$H_S = \theta_1 \exp \left(-\int_0^t \zeta(s) ds \right) + \Lambda \exp \left(-\int_0^t \zeta(s) ds \right) \times \left(\int_0^t e^{\int_0^s \zeta(u) du} ds \right) > 0.$$

Next, we can write the second equation of system (1) as

$$\frac{dH_I}{dt} \geq -\eta_I H_I,$$

and consequently

$$H_I \geq \theta_2 \exp \left(-\int_0^t \eta_I ds \right) > 0.$$

In the similar manner, from the rest of the two equations of the system (1) we may obtain

$$V_W \geq \theta_3 \exp\left(-\int_0^t \delta_V ds\right) > 0 \quad \text{and} \quad V_M \geq \theta_4 \exp\left(-\int_0^t \delta_V ds\right) > 0.$$

Thus we achieve that all the state variables H_S, H_I, V_W and V_M are non-negative. Next we study the criteria for which the state variables of the system (1) would be bounded. Combining the first two equations of the system (1), it is obtained that

$$\frac{dH_S}{dt} + \frac{dH_I}{dt} = \Lambda - \mu_S H_S - \eta_I H_I.$$

In a biologically and biomedically realistic disease system, the natural decay rate of the healthy liver cells is less than that of infected liver cells, that is $\mu_S \leq \eta_I$ and consequently

$$\frac{dH_S}{dt} + \frac{dH_I}{dt} \leq \Lambda - \mu_S (H_S + H_I).$$

Finding the limit superior on both sides,

$$\limsup_{t \rightarrow \infty} (H_S + H_I) \leq \frac{\Lambda}{\mu_S}.$$

Accordingly, we can write

$$H_S + H_I \leq \frac{\Lambda}{\mu_S}.$$

In the similar process, from the last two equations of the system (1), we get

$$V_W + V_M \leq \vartheta_V,$$

where $\vartheta_V = \min\left\{\frac{(1-\varepsilon_2)\Lambda\sigma}{\delta_V\mu_S}, \frac{(1-p\varepsilon_2)k\sigma\Lambda}{\delta_V\mu_S}\right\}$.

Therefore, it is noticeable that all the solutions (H_S, H_I, V_W, V_M) of the system (1) along with the non-negative initial condition (2) are non-negative and bounded, also the non-negativity of the solutions in consort with the boundedness implies the well-posedness of the system and the solutions are uniformly bounded. Therefore we get the feasible, positively invariant and attracting region Ω in \mathbb{R}_+^4 as

$$\Omega = \left\{ (H_S, H_I, V_W, V_M) \in \mathbb{R}_+^4 : H_S + H_I \leq \frac{\Lambda}{\mu_S}, V_W + V_M \leq \vartheta_V \right\}. \tag{3}$$

Hence the proof is completed. □

Theorem 2. *For the system (1) portraying the transmission kinetics of HCV infection, there exists a threshold parameter around the infection-free equilibrium point, namely basic reproduction number $(\mathcal{R}_0) = \frac{(1-\varepsilon_1)(1-\varepsilon_2)\beta\Lambda\sigma}{\mu_S\eta_I\delta_V}$ such that for $\mathcal{R}_0 > 1$, the system (1) has unique positive endemic steady state.*

Proof. In our proposed epidemic compartmental model, there always exists a infection-free equilibrium point $\Pi_0(\Lambda/\mu_S, 0, 0, 0)$ where HCV infection would not be present in the system (1) and the steady state is obtained by setting infected classes of the system (1) equal to zero that is $H_I = 0, V_W = 0$ and $V_M = 0$.

Next we compute the basic reproduction number of the system (1) using the next-generation matrix method (Diekmann et al., 1990; Van den Driessche and Watmough, 2002). It is notable that the infected compartments of the system (1) are H_I, V_W and V_M . At the infection-free steady state $\Pi_0(\Lambda/\mu_S, 0, 0, 0)$, the rate of appearance of new infections in the infected compartments, G and the rate of transition of infection among the infected compartments, K are defined as follows:

$$G = \begin{pmatrix} (1-\varepsilon_1)\frac{\beta\Lambda}{\mu_S}V_W \\ 0 \\ 0 \end{pmatrix} \quad \text{and} \quad K = \begin{pmatrix} \eta_I H_I \\ -(1-\varepsilon_2)\sigma H_I + \delta_V V_W \\ -(1-p\varepsilon_2)k\sigma H_I + \delta_V V_M \end{pmatrix}.$$

Next we are setting that the entry-wise non-negative new infection matrix is \mathcal{G} . Let the non-singular Metzler matrix defining the transitions of HCV infection between the infectious compartments is \mathcal{K} , and the matrices \mathcal{G}, \mathcal{K} , are given as follows:

$$\mathcal{G} = \begin{pmatrix} 0 & (1-\varepsilon_1)\frac{\beta\Lambda}{\mu_S} & 0 \\ 0 & 0 & 0 \\ 0 & 0 & 0 \end{pmatrix} \quad \text{and} \quad \mathcal{K} = \begin{pmatrix} \eta_I & 0 & 0 \\ -(1-\varepsilon_2)\sigma & \delta_V & 0 \\ -(1-p\varepsilon_2)k\sigma & 0 & \delta_V \end{pmatrix}.$$

We observe that K^{-1} is also entry-wise non-negative matrix and thus GK^{-1} is entry-wise non-negative next-generation matrix showing the expected number of new infections which is given by

$$GK^{-1} = \begin{pmatrix} \frac{(1-\varepsilon_1)(1-\varepsilon_2)\beta\Lambda\sigma}{\mu_S\eta_I\delta_V} & \frac{(1-\varepsilon_1)\beta\Lambda}{\mu_S\delta_V} & 0 \\ 0 & 0 & 0 \\ 0 & 0 & 0 \end{pmatrix}.$$

The basic reproduction number is the spectral radius of the next-generation matrix for the system (1) and thus we get

$$\mathcal{R}_0 = \frac{(1-\varepsilon_1)(1-\varepsilon_2)\beta\Lambda\sigma}{\mu_S\eta_I\delta_V}.$$

The basic reproduction number (\mathcal{R}_0) represents the average number of secondary infections in a communicable disease transmission system. While the HCV infection persists in the system, there exists unique positive endemic steady state $\Pi^*(H_S^*, H_I^*, V_W^*, V_M^*)$ given by

$$\begin{aligned} H_S^* &= \frac{\Lambda}{\mu_S} \frac{1}{\mathcal{R}_0}, & V_W^* &= \frac{\Lambda(1-\varepsilon_2)\sigma}{\eta_I\delta_V} \left(1 - \frac{1}{\mathcal{R}_0}\right), \\ H_I^* &= \frac{\Lambda}{\eta_I} \left(1 - \frac{1}{\mathcal{R}_0}\right), & V_M^* &= \frac{(1-p\varepsilon_2)k\sigma}{\eta_I\delta_V} \left(1 - \frac{1}{\mathcal{R}_0}\right). \end{aligned}$$

Therefore, it is noted that $\Pi^*(H_S^*, H_I^*, V_W^*, V_M^*)$ exists with non-negative initial condition (2) only when $\mathcal{R}_0 > 1$. Hence the proof is completed. □

4 Local Properties of the System

Theorem 3. *The system (1) is locally asymptotically stable around the infection-free equilibrium point $\Pi_0(\Lambda/\mu_S, 0, 0, 0)$ while $\mathcal{R}_0 < 1$ and is unstable if $\mathcal{R}_0 > 1$.*

Proof. The local asymptotic stability of the system (1) will be illustrated by analyzing the stability of the Jacobian matrix J_{Π_0} which is given as follows:

$$J_{\Pi_0} = \begin{pmatrix} -\mu_S & 0 & -\frac{(1-\varepsilon_1)\beta\Lambda}{\mu_S} & 0 \\ 0 & -\eta_I & \frac{(1-\varepsilon_1)\beta\Lambda}{\mu_S} & 0 \\ 0 & (1-\varepsilon_2)\sigma & -\delta_V & 0 \\ 0 & (1-p\varepsilon_2)k\sigma & 0 & -\delta_V \end{pmatrix}.$$

Characteristic equation of the Jacobian matrix J_{Π_0} corresponding to the eigenvalue λ is given by

$$(-\mu_S - \lambda)(-\delta_V - \lambda)(\lambda^2 + (\delta_V + \eta_I)\lambda + \delta_V\eta_I(1 - \mathcal{R}_0)) = 0. \tag{4}$$

The characteristic equation (4) states that two eigenvalues are real and negative ($-\mu_S$, and $-\delta_V$). The infection-free equilibrium $\Pi_0(\Lambda/\mu_S, 0, 0, 0)$ would be locally asymptotically stable if all the four eigenvalues of the characteristic equation (4) are negative or have negative real parts. This will be satisfied if $\delta_V\eta_I(1 - \mathcal{R}_0) > 0$. Therefore for $\mathcal{R}_0 < 1$, the quadratic equation $\lambda^2 + (\delta_V + \eta_I)\lambda + \delta_V\eta_I(1 - \mathcal{R}_0)$ has two strictly real and negative roots or roots having negative real parts. Thus $\Pi_0(\Lambda/\mu_S, 0, 0, 0)$ is locally asymptotically stable for $\mathcal{R}_0 < 1$ (see Figure 7) and otherwise unstable. Hence the proof is completed. □

Theorem 4. *While basic reproduction number, $\mathcal{R}_0 = 1$, the system (1) experiences transcritical bifurcation at the infection-free steady state $\Pi_0(\Lambda/\mu_S, 0, 0, 0)$ along with the bifurcation threshold $\mathcal{R}_0 = 1$.*

Proof. Let us consider that $x_1 \equiv H_S, x_2 \equiv H_I, x_3 \equiv V_W, x_4 \equiv V_M$, and we can arrange the system equation (1) into the following form:

$$\mathcal{D}(x_1, x_2, x_3, x_4; \beta) = \begin{pmatrix} \Lambda - (1-\varepsilon_1)\beta x_1 x_3 - \mu_S x_1 \\ (1-\varepsilon_1)\beta x_1 x_3 - \eta_I x_2 \\ (1-\varepsilon_2)\sigma x_2 - \delta_V x_3 \\ (1-p\varepsilon_2)k\sigma x_2 - \delta_V x_4 \end{pmatrix} \equiv \begin{pmatrix} f_1 \\ f_2 \\ f_3 \\ f_4 \end{pmatrix}, \tag{5}$$

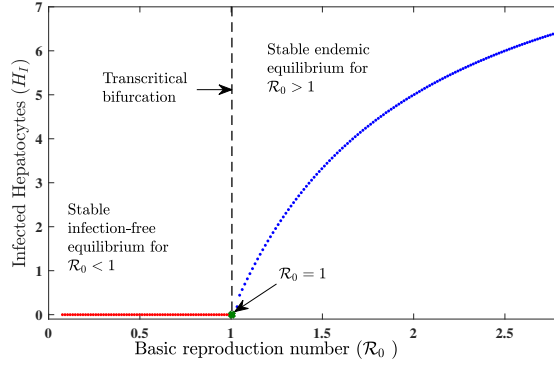


Figure 2: Transcritical bifurcation diagram of infected liver cells with \mathcal{R}_0 . Baseline parameter values are same as given in Table 1 and we have varied the value of β in $(0.0005, 0.02)$.

considering β_0 as bifurcation threshold parameter at $\mathcal{R}_0 = 1$, where $\beta_0 = \frac{\mu_S \eta_I \delta_V}{(1-\varepsilon_1)(1-\varepsilon_2)\Lambda\sigma}$. At $\mathcal{R}_0 = 1$, the Jacobian matrix around the infection-free equilibrium (Π_0) is computed as,

$$J_{\beta_0} = \begin{pmatrix} -\mu_S & 0 & -\frac{\eta_I \delta_V}{(1-\varepsilon_2)\sigma} & 0 \\ 0 & -\eta_I & \frac{\eta_I \delta_V}{(1-\varepsilon_2)\sigma} & 0 \\ 0 & (1-\varepsilon_2)\sigma & -\delta_V & 0 \\ 0 & (1-p\varepsilon_2)k\sigma & 0 & -\delta_V \end{pmatrix}.$$

We find that $-\mu_S, -\delta_V, 0$, and $-(\eta_I + \delta_V)$ are the four eigenvalues corresponding to the Jacobian matrix J_{β_0} . Next we investigate whether Sotomayor’s Theorem (Perko, 2013) is applicable to prove the existence of transcritical bifurcation at Π_0 .

Let us consider that, with respect to the eigenvalue zero, $y = [y_1 \ y_2 \ y_3 \ y_4]^T$ and $z = [z_1 \ z_2 \ z_3 \ z_4]^T$ are the right eigenvector and left eigenvector, respectively, where

$$y = \left[-\frac{\eta_I}{\mu_S} \quad 1 \quad \frac{(1-\varepsilon_2)\sigma}{\delta_V} \quad \frac{(1-p\varepsilon_2)k\sigma}{\delta_V} \right]^T y_2 \quad \text{and} \quad z = \left[0 \quad 1 \quad 0 \quad \frac{\eta_I}{(1-\varepsilon_2)\sigma} \right]^T z_2.$$

Now we differentiate the system (5) with respect to β around $\Pi_0(\Lambda/\mu_S, 0, 0, 0)$, and we obtain $\mathcal{D}^\beta(\Pi_0; \beta) = (0 \ 0 \ 0 \ 0)^T$. Therefore we get

$$y^T \mathcal{D}^\beta(\Pi_0; \beta) = \left[-\frac{\eta_I}{\mu_S} \quad 1 \quad \frac{(1-\varepsilon_2)\sigma}{\delta_V} \quad \frac{(1-p\varepsilon_2)k\sigma}{\delta_V} \right] y_2 [0 \ 0 \ 0 \ 0]^T$$

and consequently

$$\Delta_1 = y^T \mathcal{D}^\beta(\Pi_0; \beta) = 0.$$

Hence the first condition of Sotomayor’s Theorem is satisfied. Now we investigate if the second condition of Sotomayor’s Theorem would be satisfied and to check this, let us consider that

$$\begin{aligned} \Delta_2 &= \sum_{i,j=1}^4 z_i y_j \left[\frac{\partial^2 f_i}{\partial x_j \partial \beta}(\Pi_0) \right]_{\beta=\beta_0} = \sum_{j=1}^4 z_2 y_j \left[\frac{\partial}{\partial x_j} \{ (1-\varepsilon_1)x_1 x_3 \}(\Pi_0) \right]_{\beta=\beta_0} \\ &= \frac{(1-\varepsilon_1)(1-\varepsilon_2)\sigma\Lambda}{\delta_V \mu_S} z_2 y_2 > 0. \end{aligned}$$

Thus $\Delta_2 \neq 0$ and as a result the second condition of Sotomayor’s Theorem is satisfied. Finally, let us consider that

$$\begin{aligned} \Delta_3 &= \sum_{i,j,l=1}^4 z_i y_j y_l \left[\frac{\partial^2 f_i}{\partial x_j \partial x_l}(\Pi_0) \right]_{\beta=\beta_0} = \sum_{j,l=1}^4 z_2 y_j y_l \left[\frac{\partial^2 f_2}{\partial x_j \partial x_l}(\Pi_0) \right]_{\beta=\beta_0} \\ &= -\frac{2(1-\varepsilon_1)(1-\varepsilon_2)\beta_0 \eta_I \sigma}{\mu_S \delta_V} z_2 y_2^2 < 0. \end{aligned}$$

Therefore it is observed that $\Delta_3 \neq 0$. Thus the third condition of Sotomayor’s Theorem is also satisfied. Hence it can be concluded that a transcritical bifurcation occurs in the system (1) around the infection-free equilibrium (Π_0) at $\mathcal{R}_0 = 1$. \square

The Figure 2 is indicating that the model (1) experiences transcritical bifurcation at $\mathcal{R}_0 = 1$ around the infection-free equilibrium. We choose the transmission rate (β) as the threshold parameter for bifurcation. The stability of the infection-free equilibrium alters from stability to instability (for $\mathcal{R}_0 > 1$) when it crosses $\mathcal{R}_0 = 1$.

Theorem 5. *The system (1) is locally asymptotically stable around the endemic equilibrium point $\Pi^*(H_S^*, H_I^*, V_W^*, V_M^*)$ while $\mathcal{R}_0 > 1$ and is unstable if $\mathcal{R}_0 < 1$.*

Proof. The Jacobian matrix computed at the endemic steady state $\Pi^*(H_S^*, H_I^*, V_W^*, V_M^*)$ is

$$J_{\Pi^*} = \begin{pmatrix} -(1 - \varepsilon_1)\beta V_W^* - \mu_S & 0 & -(1 - \varepsilon_1)\beta H_S^* & 0 \\ (1 - \varepsilon_1)\beta V_W^* - \mu_S & -\eta_I & (1 - \varepsilon_1)\beta H_S^* & 0 \\ 0 & (1 - \varepsilon_2)\sigma & -\delta_V & 0 \\ 0 & (1 - p\varepsilon_2)k\sigma & 0 & -\delta_V \end{pmatrix}.$$

The characteristic equation of the matrix J_{Π^*} corresponding to the eigenvalue ψ is given as

$$\psi^4 + \zeta_3\psi^3 + \zeta_2\psi^2 + \zeta_1\psi + \zeta_0 = 0, \tag{6}$$

where

$$\begin{aligned} \zeta_3 &= \eta_I + 2\delta_V + \mu_S + \mu_S(\mathcal{R}_0 - 1), \\ \zeta_2 &= \delta_V^2 + \eta_I\delta_V + \mu_S(\eta_I + 2\delta_V) + \mu_S(\eta_I + 2\delta_V)(\mathcal{R}_0 - 1), \\ \zeta_1 &= \mu_S(\delta_V^2 + \eta_I\delta_V) + \mu_S(\delta_V^2 + 2\delta_V\eta_I)(\mathcal{R}_0 - 1), \\ \zeta_0 &= \mu_S\eta_I\delta_V^2(\mathcal{R}_0 - 1). \end{aligned}$$

Now the Routh-Hurwitz Criterion (Routh, 1877; Hurwitz et al., 1964; Gantmacher and Brenner, 2005), viz, $\zeta_3 > 0, \zeta_0 > 0, \zeta_3\zeta_2 - \zeta_1 > 0$ and $(\zeta_3\zeta_2 - \zeta_1)\zeta_1 - \zeta_3^2\zeta_0 > 0$ for the equation (6) is satisfied for $\mathcal{R}_0 > 1$ and consequently $\Pi^*(H_S^*, H_I^*, V_W^*, V_M^*)$ is locally asymptotically stable in this regard (see Figure 8). \square

5 Global Stability of the System Around Endemic Equilibrium

In this Section, we analyse the global stability of the unique endemic equilibrium $\Pi^*(H_S^*, H_I^*, V_W^*, V_M^*)$ under the condition $\mathcal{R}_0 > 1$. In this regard, we use a specific Lyapunov function similarly used by Korobeinikov and Maini (2004), McCluskey (2010), and Samui et al. (2020). Such Lyapunov function provides advantages of the properties of the function:

$$\mathfrak{g}(o) = o - 1 - \ln(o). \tag{7}$$

The above function is non-negative in \mathbb{R}_+^4 except at $o = 1$, where it attains the value zero. Next we study the global stability of Π^* using the following theorem.

Theorem 6. *Let $\mathcal{R}_0 > 1$. The endemic equilibrium $\Pi^*(H_S^*, H_I^*, V_W^*, V_M^*)$ exists and around it, the system (1) is globally asymptotically stable in the interior of \mathbb{R}_+^4 .*

Proof. We consider that $\mathcal{R}_0 > 1$ and the endemic equilibrium $\Pi^*(H_S^*, H_I^*, V_W^*, V_M^*)$ exists. Let us consider the following Lyapunov function which is well-defined in the interior of \mathbb{R}_+^4 and is defined as

$$\mathcal{V}_{\Pi^*}(H_S, H_I, V_W, V_M) = H_S^*\mathfrak{g}\left(\frac{H_S}{H_S^*}\right) + H_I^*\mathfrak{g}\left(\frac{H_I}{H_I^*}\right) + V_W^*\mathfrak{g}\left(\frac{V_W}{V_W^*}\right) + V_M^*\mathfrak{g}\left(\frac{V_M}{V_M^*}\right). \tag{8}$$

We need to show that $\dot{\mathcal{C}}_{\Pi^*}$ is always negative definite. Differentiating \mathcal{C}_{Π^*} along the solution trajectory of the system (1), we get

$$\begin{aligned}
 \dot{\mathcal{C}}_{\Pi^*} &= \dot{H}_S \left(1 - \frac{H_S^*}{H_S}\right) + \dot{H}_I \left(1 - \frac{H_I^*}{H_I}\right) + \dot{V}_W \left(1 - \frac{V_W^*}{V_W}\right) + \dot{V}_M \left(1 - \frac{V_M^*}{V_M}\right) \\
 &= [\Lambda - (1 - \varepsilon_1)\beta H_S V_W - \mu_S H_S] \left(1 - \frac{H_S^*}{H_S}\right) + [(1 - \varepsilon_1)\beta H_S V_W - \eta_I H_I] \left(1 - \frac{H_I^*}{H_I}\right) \\
 &\quad + [(1 - \varepsilon_2)\sigma H_I - \delta_V V_W] \left(1 - \frac{V_W^*}{V_W}\right) + [(1 - p\varepsilon_2)k\sigma H_I - \delta_V V_M] \left(1 - \frac{V_M^*}{V_M}\right) \\
 &= \Lambda - (1 - \varepsilon_1)\beta H_S V_W - \mu_S H_S - \Lambda \frac{H_S^*}{H_S} + (1 - \varepsilon_1)\beta H_S V_W \frac{H_S^*}{H_S} + \mu_S H_S^* \\
 &\quad + (1 - \varepsilon_1)\beta H_S V_W - \eta_I H_I - (1 - \varepsilon_1)\beta H_S V_W \frac{H_I^*}{H_I} + \eta_I H_I^* + (1 - \varepsilon_2)\sigma H_I - \delta_V V_W \\
 &\quad - (1 - \varepsilon_2)\sigma H_I \frac{V_W^*}{V_W} + \delta_V V_W^* + (1 - p\varepsilon_2)k\sigma H_I - \delta_V V_M - (1 - p\varepsilon_2)k\sigma H_I \frac{V_M^*}{V_M} + \delta_V V_M^* \\
 &= (1 - \varepsilon_1)\beta H_S^* V_W^* + \mu_S H_S^* - (1 - \varepsilon_1)\beta H_S V_W - \mu_S H_S - (1 - \varepsilon_1)\beta H_S^2 V_W^* \\
 &\quad + (1 - \varepsilon_1)\beta H_S V_W \frac{H_S^*}{H_S} + \mu_S H_S^* + (1 - \varepsilon_1)\beta H_S V_W - (1 - \varepsilon_1)\beta H_S^* V_W^* \frac{H_I}{H_I^*} \\
 &\quad - (1 - \varepsilon_1)\beta H_S V_W \frac{H_I^*}{H_I} + (1 - \varepsilon_1)\beta H_S^* V_W^* - \mu_S \frac{H_S^2}{H_S} \\
 &\quad + (1 - \varepsilon_2)\sigma H_I - (1 - \varepsilon_2)\sigma H_I^* \frac{V_W}{V_W^*} - (1 - \varepsilon_2)\sigma H_I \frac{V_W^*}{V_W} + (1 - \varepsilon_2)\sigma H_I^* \\
 &\quad + (1 - p\varepsilon_2)k\sigma H_I - (1 - p\varepsilon_2)k\sigma H_I^* \frac{V_M}{V_M^*} - (1 - p\varepsilon_2)k\sigma H_I \frac{V_M^*}{V_M} + (1 - p\varepsilon_2)k\sigma H_I^* \\
 &= \mu_S H_S^* \left(2 - \frac{H_S^*}{H_S} - \frac{H_S}{H_S^*}\right) + (1 - \varepsilon_1)H_S^* V_W^* \left(2 - \frac{H_S^*}{H_S} - \frac{H_I}{H_I^*}\right) \\
 &\quad + (1 - \varepsilon_2)\sigma H_I \left(3 - \frac{H_I^*}{H_I} - \frac{V_W}{V_W^*} - \frac{H_I V_W}{H_I^* V_W^*}\right) - H_I^* \sigma (1 - p\varepsilon_2)k \left(\frac{1}{V_M^*} - 1\right) \\
 &\quad - \sigma (1 - \varepsilon_2) \left(H_I - 2H_I^*\right) - (1 - p\varepsilon_2)k\sigma \frac{H_I V_M^*}{V_M} - (1 - \varepsilon_1)\beta H_S V_W \frac{H_I^*}{H_I}.
 \end{aligned}$$

From the above expression, using the relation of geometric and arithmetic means (i.e., arithmetic mean is greater than or equal to geometric mean), it is obtained that $(2 - \frac{H_S^*}{H_S} - \frac{H_S}{H_S^*}) \leq 0$, $(2 - \frac{H_S^*}{H_S} - \frac{H_I}{H_I^*}) \leq 0$, $(3 - \frac{H_I^*}{H_I} - \frac{V_W}{V_W^*} - \frac{H_I V_W}{H_I^* V_W^*}) \leq 0$, and thus we get $\dot{\mathcal{C}}_{\Pi^*} \leq 0$, if $H_I \geq 2H_I^*$ and $V_M^* \leq 1$; the equality holds only at Π^* . Therefore, $\Pi^*(H_S^*, H_I^*, V_W^*, V_M^*)$ is globally asymptotically stable (see Figure 10) and the proof is completed. \square

6 Sensitivity Analysis

Sensitivity analysis is performed to explore the robustness of the basic reproduction number, \mathcal{R}_0 to measure the fluctuations and relative changes in the baseline parameters associated to the basic reproduction number (Chowdhury et al., 2016). Sensitivity analysis helps to identify the influence of the parameters on the basic reproduction number and in the transmission of Hepatitis C virus infection. The knowledge about the impact of the baseline parameters when a relative change is triggered to these parameter values assists to determine appropriate intervention strategies.

Table 2: Sensitivity indices of the basic reproduction number (\mathcal{R}_0) with respect to the model parameters, evaluated at the baseline parameter values listed in the Table 1.

Parameter	μ_S	η_I	σ	ε_1	β	δ_V	Λ	ε_2
Index Value	-1.0000	-1.0000	+1.0000	-0.8691	+1.00004	-1.0000	+1.0000	-0.9417

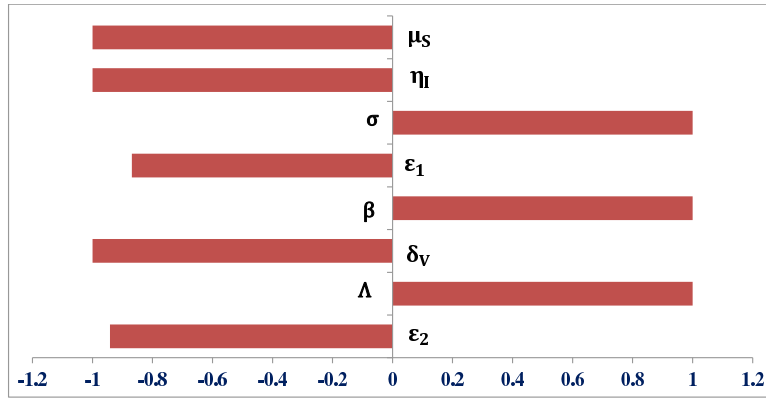


Figure 3: The figure shows tornado plot regarding the sensitivity indices of \mathcal{R}_0 .

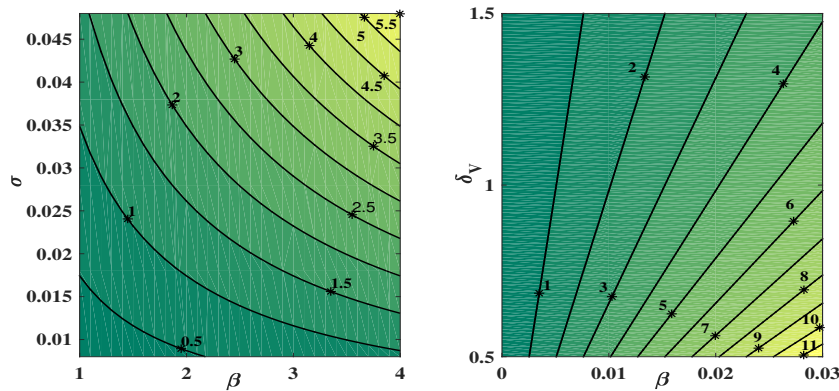


Figure 4: The figure is depicting the contour plots of \mathcal{R}_0 for the most sensitive parameters, the transmission rate (β) versus the production rate of both wild and mutant virus (σ) (in the left panel) and the removal rate of both wild and mutant virus (δ_V) (in the right panel), rest of the parameter values are taken from Table 1.

The normalized forward sensitivity indices of \mathcal{R}_0 with respect to parameters associated to \mathcal{R}_0 are given as follows:

$$\begin{aligned}
 Y_{\epsilon_1}^{\mathcal{R}_0} &= \frac{\partial \mathcal{R}_0}{\partial \epsilon_1} \times \frac{\epsilon_1}{\mathcal{R}_0} = -\frac{(1 - \epsilon_2)\beta\Lambda\sigma}{\mu_S\eta_I\delta_V} \times \frac{\epsilon_1}{\mathcal{R}_0}, \\
 Y_{\epsilon_2}^{\mathcal{R}_0} &= \frac{\partial \mathcal{R}_0}{\partial \mu} \times \frac{\epsilon_2}{\mathcal{R}_0} = -\frac{(1 - \epsilon_1)\beta\Lambda\sigma}{\mu_S\eta_I\delta_V} \times \frac{\epsilon_2}{\mathcal{R}_0}, \\
 Y_{\beta}^{\mathcal{R}_0} &= \frac{\partial \mathcal{R}_0}{\partial \mu} \times \frac{\beta}{\mathcal{R}_0} = \frac{(1 - \epsilon_1)(1 - \epsilon_2)\Lambda\sigma}{\mu_S\eta_I\delta_V} \times \frac{\beta}{\mathcal{R}_0}, \\
 Y_{\Lambda}^{\mathcal{R}_0} &= \frac{\partial \mathcal{R}_0}{\partial \mu} \times \frac{\Lambda}{\mathcal{R}_0} = \frac{(1 - \epsilon_1)(1 - \epsilon_2)\beta\sigma}{\mu_S\eta_I\delta_V} \times \frac{\Lambda}{\mathcal{R}_0}, \\
 Y_{\sigma}^{\mathcal{R}_0} &= \frac{\partial \mathcal{R}_0}{\partial \mu} \times \frac{\sigma}{\mathcal{R}_0} = \frac{(1 - \epsilon_1)(1 - \epsilon_2)\beta\Lambda}{\mu_S\eta_I\delta_V} \times \frac{\sigma}{\mathcal{R}_0}, \\
 Y_{\mu_S}^{\mathcal{R}_0} &= \frac{\partial \mathcal{R}_0}{\partial \mu} \times \frac{\mu_S}{\mathcal{R}_0} = -\frac{(1 - \epsilon_1)(1 - \epsilon_2)\beta\Lambda\sigma}{\mu_S^2\eta_I\delta_V} \times \frac{\mu_S}{\mathcal{R}_0}, \\
 Y_{\eta_I}^{\mathcal{R}_0} &= \frac{\partial \mathcal{R}_0}{\partial \mu} \times \frac{\eta_I}{\mathcal{R}_0} = -\frac{(1 - \epsilon_1)(1 - \epsilon_2)\beta\Lambda\sigma}{\mu_S\eta_I\delta_V^2} \times \frac{\eta_I}{\mathcal{R}_0}, \\
 Y_{\delta_V}^{\mathcal{R}_0} &= \frac{\partial \mathcal{R}_0}{\partial \mu} \times \frac{\delta_V}{\mathcal{R}_0} = -\frac{(1 - \epsilon_1)(1 - \epsilon_2)\beta\Lambda\sigma}{\mu_S\eta_I\delta_V^2} \times \frac{\delta_V}{\mathcal{R}_0}.
 \end{aligned}$$

Figure 3 shows the tornado plot of partial rank correlation coefficient (PRCC) sensitivity analysis. All relevant parameters

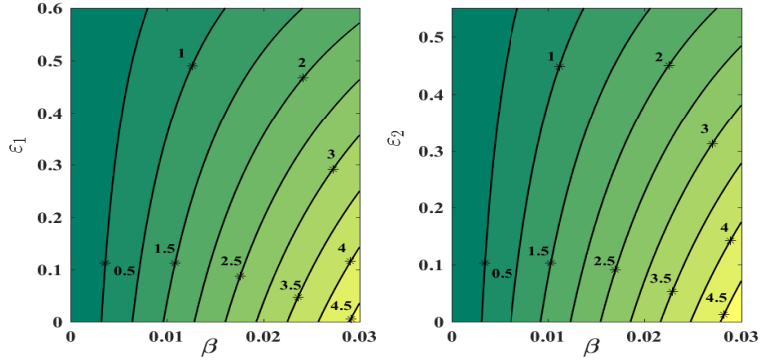


Figure 5: The figure is depicting the contour plots of \mathcal{R}_0 for the most sensitive parameter, the HCV infection transmission rate (β) versus the control of SOF (ε_1) (in the left panel) and the control of VEL (ε_2) (in the right panel), rest of the parameter values are taken from Table 1.

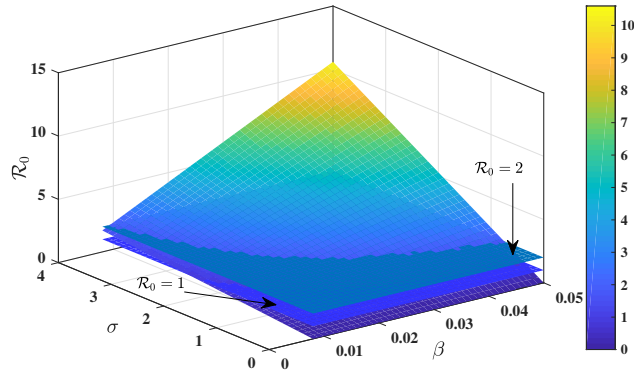


Figure 6: The figure indicates the changes of the value of the basic reproduction number (\mathcal{R}_0) when the disease transmission rate (β) and the virions production rate (σ) vary simultaneously in our system (1). The parametric values are same as in Table 1.

are varied against \mathcal{R}_0 throughout the range given in Table 1. Parameters with $PRCCs > 0$ will increase \mathcal{R}_0 when they would be increased, while the parameters with $PRCCs < 0$ will decrease \mathcal{R}_0 when the corresponding parameters would be increased. From this figure, it could be seen that $\sigma, \beta, \Lambda, \mu_s, \eta_I$ and δ_V play the most significant role to control the HCV infection and these are the variables that have the largest impact on the outcome. From the sensitivity analysis, the numerical simulation suggests that control of HCV infection is most likely to be achieved by lowering the values of Λ, β, σ . On the other hand, increasing $\mu_s, \eta_I, \delta_V, \varepsilon_1, \varepsilon_2$ is unlikely to eradicate the infection.

Figure 4 shows that as infection rate (β) or the production rate of virions (σ) increases, the system changes from an infection-free state to an endemic state. Also, it is clearly observed that as the removal rate of virus (δ_V) increases, the systems switches from endemic to infection-free state. Figure 5 shows the role of drug effectiveness to control the disease. This figure shows that increasing the value of drug efficiency reduces the value of \mathcal{R}_0 and for certain threshold value, the system switches to an infection-free state from an endemic state.

In Figure 6, following the colorbar scheme, we determine the surface \mathcal{R}_0 , the surface $\mathcal{R}_0 = 1$ and the surface $\mathcal{R}_0 = 2$ varying the transmission rate (β) and the virions production rate (σ). When the transmission rate (β) decreases, \mathcal{R}_0 will decrease and reach below 1, thus the system attains its infection-free state. Also we can control \mathcal{R}_0 by reducing virions production rate (σ). Hence we can expect that DAA (combination of SOF/VEL) can play a pivotal role to control the disease progression.

7 Optimal Control Approach

Inside this Section, an optimal control problem is exhibited considering the performance of the two drugs SOF and VEL on the controlled model equations. Here our target is to minimize the number of infected liver cells, virus strains as well as the cost of implemented control strategies ($u_1(t), u_2(t)$).

- First control function $u_1(t)$ stands for the effect of antiviral drug dose of SOF which helps to block the spreading of infection.
- Second control function $u_2(t)$ stands for the effect of antiviral drug dose of VEL which helps to block the production of viral particles.

The control problem consists of a system of four nonlinear differential equations given as below:

$$\begin{aligned}\frac{dH_S}{dt} &= \Lambda - (1 - u_1(t))\beta H_S V_W - \mu_S H_S, \\ \frac{dH_I}{dt} &= (1 - u_1(t))\beta H_S V_W - \eta_I H_I, \\ \frac{dV_W}{dt} &= (1 - u_2(t))\sigma H_I - \delta_V V_W, \\ \frac{dV_M}{dt} &= (1 - pu_2(t))k\sigma H_I - \delta_V V_M,\end{aligned}\tag{9}$$

subject to the non-negative initial condition (2).

The objective functional $\mathcal{F}(u(t))$ for the control problem is defined as

$$\mathcal{F}(u(t)) = \int_{t_0}^{t_f} \left[P_1 H_I + P_2 V_W + P_3 V_M + \frac{1}{2} \left(Q_1 u_1^2(t) + Q_2 u_2^2(t) \right) \right] dt.\tag{10}$$

This objective functional includes the terms H_I (infected populations), V_W and V_M (wild and mutant virus populations) that should be minimized. $Q_1 u_1^2(t)$ denotes cost for antiviral drug SOF that blocks infection, $Q_2 u_2^2(t)$ represents the cost of antiviral drug VEL that blocks of production of viral particles. The positive balancing and optimal control regularizing coefficients are P_1, P_2, P_3, Q_1 , and Q_2 . Therefore our aim is to seek the optimal controls $u_1^*(t)$ and $u_2^*(t)$ such that

$$\mathcal{F}(u_1^*(t), u_2^*(t)) = \min\{\mathcal{F}(u_1(t), u_2(t))\},$$

subject to system (9) and

$$\Gamma = \{(u_1(t), u_2(t)) : 0 \leq u_1(t), u_2(t) \leq 1, \forall t \in [t_0, t_f]\},$$

where Γ is the control set. The basic framework of an optimal control problem is to prove the existence of the optimal control and then characterize the optimal control through optimality system (Pontryagin, 2018). We prove the existence of optimal control problem given in (9) using the approach of Fleming and Rishel (2012) and then characterize it for optimality.

7.1 Existence of Optimal Control

The existence condition of the optimal control can be verified by using the results of Fleming and Rishel (2012) and of Lukes (1982). To prove the existence of optimal control problem, we have to prove the following conditions:

- The set of controls and corresponding state variables are non-empty.
- The control set Γ is convex and closed.
- The right-hand side of the state system is bounded by a linear function in the state and control variables.
- The integrand of the objective functional (10), $\mathcal{L}(H_S, H_I, V_W, V_M)$ is convex on Γ .
- The integrand of the objective functional is bounded below by $\kappa_1 [(u_1(t))^2 + (u_2(t))^2]^{\tau/2} \kappa_2$, where $\kappa_1 > 0$, $\kappa_2 > 0$ and $\tau > 1$.

In our presented optimal controlled model system (9), H_S, H_I, V_W, V_M are the state variables, and $u_1(t), u_2(t)$ are the control variables. Next we state and prove the following theorem.

Theorem 7. *There exists an optimal control variable $u^*(t) = (u_1^*(t), u_2^*(t)) \in \Gamma$ such that*

$$\mathcal{F}(u_1^*(t), u_2^*(t)) = \min\{\mathcal{F}(u_1(t), u_2(t))\}.$$

Proof. Using the result of Boyce and DiPrima (2012, see Theorem 7.1.1) we can prove that the set of control and the corresponding variables are non-empty. Let

$$\begin{aligned} \dot{H}_S &= \phi_1(t, H_S, H_I, V_W, V_M), & \dot{V}_W &= \phi_3(t, H_S, H_I, V_W, V_M), \\ \dot{H}_I &= \phi_2(t, H_S, H_I, V_W, V_M), & \dot{V}_M &= \phi_4(t, H_S, H_I, V_W, V_M), \end{aligned}$$

where $\phi_1, \phi_2, \phi_3, \phi_4$ are the right-hand side of the system (9). Here the right-hand side of the state system is continuous, is bounded above by a sum of the bounded control and the state, and can be written as a linear function of u_1, u_2 with coefficients depending on time and the state variables. Thus H_S, H_I, V_W, V_M are all continuous. Then $\phi_1, \phi_2, \phi_3,$ and ϕ_4 are also continuous and the partial derivatives $\frac{\partial \phi_1}{\partial H_S}, \frac{\partial \phi_1}{\partial H_I}, \frac{\partial \phi_1}{\partial V_W}, \frac{\partial \phi_1}{\partial V_M}, \frac{\partial \phi_2}{\partial H_S}, \frac{\partial \phi_2}{\partial H_I}, \frac{\partial \phi_2}{\partial V_W}, \frac{\partial \phi_2}{\partial V_M}, \frac{\partial \phi_3}{\partial H_S}, \frac{\partial \phi_3}{\partial H_I}, \frac{\partial \phi_3}{\partial V_W}, \frac{\partial \phi_3}{\partial V_M}, \frac{\partial \phi_4}{\partial H_S}, \frac{\partial \phi_4}{\partial H_I}, \frac{\partial \phi_4}{\partial V_W}, \frac{\partial \phi_4}{\partial V_M}$ are all continuous. Hence the solution of control is unique and the corresponding state variables are non-empty.

The controls $u_1(t), u_2(t)$ and state variables H_S, H_I, V_W, V_M of the system (10) are non-negative. Hence the necessary convexity of our objective functional stated in terms of $u_1(t), u_2(t)$ is satisfied.

According to the definition, the sets of admissible Lebesgue measurable control variables $(u_1(t), u_2(t)) \in \Gamma$ along with $(u_1(t), u_2(t)) \in \mathcal{U}$ are convex and closed.

The boundedness of the optimal control system determines the compactness needed for the existence of optimal control (Birkhoff and Rota, 1962). To verify this argument we rewrite the system (9) in the form

$$X' = AX + F(X),$$

where $X = [H_S, H_I, V_W, V_M]^T$,

$$F(X) = \begin{pmatrix} \Lambda - (1 - u_1(t))\beta H_S V_W \\ (1 - u_1(t))\beta H_S V_W \\ 0 \\ 0 \end{pmatrix} \quad \text{and} \quad A = \begin{pmatrix} -\mu_S & 0 & 0 & 0 \\ 0 & -\eta_I & 0 & 0 \\ 0 & (1 - u_2(t))\sigma & -\delta_V & 0 \\ 0 & (1 - pu_2(t))k\sigma & 0 & -\delta_V \end{pmatrix},$$

and X' denotes the derivative of X with respect to time t . Now it is notable that system (9) is a non-linear system with bounded coefficients and on finite time interval, solutions would be bounded, then following the methods of Lukes (1982) we can set,

$$\Psi(X) = AX + F(X).$$

The term $F(X)$ satisfies

$$\begin{aligned} |F(X_1) - F(X_2)| &\leq C_1(|H_{1S}(t) - H_{2S}(t)|) + C_2(|H_{1I}(t) - H_{2I}(t)|) \\ &\quad + C_3(|V_{1W}(t) - V_{2W}(t)|) + C_4(|V_{1M}(t) - V_{2M}(t)|) \\ &\leq C(|H_{1S}(t) - H_{2S}(t)| + |H_{1I}(t) - H_{2I}(t)| + |V_{1W}(t) - V_{2W}(t)| + |V_{1M}(t) - V_{2M}(t)|), \end{aligned}$$

where the positive constant $C = \max\{C_r, \text{ for } r = 1, \dots, 4\}$ is independent of the state variables. Also we have $\Psi(X_1) - \Psi(X_2) \leq C|X_1 - X_2|$, where $C = \sum_{r=1}^4 C_r + \|\mathcal{H}\| < \infty$. So, it follows that the function Ψ is uniformly Lipchitz continuous. From the definition of control variables and non-negative initial condition we can see that a solution of the system (9) exists (Birkhoff and Rota, 1962).

The integrand of the objective functional (10) which is given by the following equation

$$\mathcal{L}(H_S, H_I, u_1, u_2) = P_1 H_I + P_2 V_W + P_3 V_M + \frac{1}{2} (Q_1 u_1^2(t) + Q_2 u_2^2(t)),$$

is convex in the control set Γ . We must verify the condition that there exists a constant $\tau > 1$ and positive numbers $\kappa_1, \kappa_2 > 0$ such that

$$\begin{aligned} \mathcal{L}(H_S, H_I, u_1, u_2) &= P_1 H_I + P_2 V_W + P_3 V_M + \frac{1}{2} (Q_1 u_1^2(t) + Q_2 u_2^2(t)) \\ &\geq \frac{1}{2} (Q_1 u_1^2(t) + Q_2 u_2^2(t)), \\ \Rightarrow \frac{1}{2} (Q_1 u_1^2(t) + Q_2 u_2^2(t)) &\geq \kappa_1 (u_1^2(t) + u_2^2(t))^{\tau/2} - \kappa_2. \end{aligned}$$

Let $\kappa_1 = \inf\{\frac{Q_1}{2}, \frac{Q_2}{2}\}$ and $\kappa_2 = 2 \sup_{t \in [t_0, t_f]} (H_I, V_W, V_M)$ and $\tau = 2$. Then it follows that

$$\mathcal{L}(H_S, H_I, u_1, u_2) \geq \kappa_1 (|u_1|^2 + |u_2|^2)^{\frac{\tau}{2}} - \kappa_2.$$

Hence the optimal control pair exists and this ends the proof. □

7.2 Characteristic of Optimal Control

The optimal control $u^*(t)$ stands for the proportion of drug usage at any instant t . To minimize cost function (10) subject to the system of ODEs (9), we now present the necessary conditions for which an optimal control and corresponding states must satisfy come from the Pontryagin’s Maximum Principle (Pontryagin, 2018). We use the Pontryagin’s Maximum Principle (PMP) to determine the optimal controls $u_1^*(t)$ and $u_2^*(t)$. By using this principle we convert the system (9) and the cost function (10) into a problem of minimizing pointwise Hamiltonian function \mathcal{H} with respect to $(u_1(t), u_2(t))$. The Hamiltonian is formed by the adjoint variables along with corresponding state variables and combining the results with the objective functional. The Hamiltonian is given by

$$\mathcal{H} = P_1 H_I + P_2 V_W + P_3 V_M + \frac{1}{2} \left(Q_1 u_1^2(t) + Q_2 u_2^2(t) \right) + \sum_{r=1}^4 \xi_r R_r, \tag{11}$$

where $\xi_1, \xi_2, \xi_3, \xi_4$ are the adjoint functions associated with the state equation in (9). $R_r, r = 1, \dots, 4$ is the right-hand side of the differential equations of r^{th} state variable in system (9). The expanded form of Hamiltonian function in (11) is given by

$$\begin{aligned} \mathcal{H} = & P_1 H_I + P_2 V_W + P_3 V_M + \frac{1}{2} \left(Q_1 u_1^2(t) + Q_2 u_2^2(t) \right) \\ & + \xi_1 \{ \Lambda - (1 - u_1(t)) \beta H_S V_W - \mu_S H_S \} + \xi_2 \{ (1 - u_1(t)) \beta H_S V_W - \eta_I H_I \} \\ & + \xi_3 \{ (1 - u_2(t)) \sigma H_I - \delta_V V_W \} + \xi_4 \{ (1 - p u_2(t)) k \sigma H_I - \delta_V V_M \}. \end{aligned} \tag{12}$$

The optimality equations are obtained when taking the partial derivatives of the Hamiltonian function \mathcal{H} with respect to the control variables $u_1(t), u_2(t)$ respectively and the time derivative of adjoint equation, $\xi'(t)$ which is obtained by taking the negative partial derivative of \mathcal{H} with respect to the model state variables $x(t)$ such that $\xi'(t) = -\mathcal{H}_x$.

Theorem 8. *There exists an optimal control set $(u_1^*(t), u_2^*(t))$ and its corresponding state solutions $H_S^*, H_I^*, V_W^*, V_M^*$ that minimize $\mathcal{J}(u_1(t), u_2(t))$, and therefore there exist adjoint functions $\xi_1, \xi_2, \xi_3, \xi_4$ such that*

$$\begin{aligned} \frac{d\xi_1}{dt} &= (1 - u_1(t)) \beta V_W (\xi_1 - \xi_2) + \xi_1 \mu_S, \\ \frac{d\xi_2}{dt} &= -P_1 + \xi_2 \eta_I - \{ \xi_3 (1 - u_2(t)) + \xi_4 (1 - p u_2(t)) k \} \sigma, \\ \frac{d\xi_3}{dt} &= -P_2 + (1 - u_1(t)) \beta H_S (\xi_1 - \xi_2) + \xi_3 \delta_V, \\ \frac{d\xi_4}{dt} &= -P_3 + \xi_4 \delta_V, \end{aligned}$$

with transversality conditions: $\xi_1(t_f) = 0, \xi_2(t_f) = 0, \xi_3(t_f) = 0, \xi_4(t_f) = 0$, and the control variables $u_1^*(t), u_2^*(t)$ satisfy the following optimality conditions:

$$\begin{aligned} u_1^*(t) &= \min \left\{ \max \left\{ 0, \frac{(\xi_2 - \xi_1) \beta H_S V_W}{Q_1} \right\}, 1 \right\}, \\ u_2^*(t) &= \min \left\{ \max \left\{ 0, \frac{(\xi_3 + k p \xi_4) \sigma H_I}{Q_2} \right\}, 1 \right\}. \end{aligned}$$

Proof. The differential equations for the adjoint functions are standard results from Pontryagin’s Maximum Principle (PMP) (Pontryagin, 2018). For the given the Hamiltonian function in (12), the adjoint equations can be easily computed by

$$\frac{d\xi_1}{dt} = -\frac{\partial \mathcal{H}}{\partial H_S}, \quad \frac{d\xi_2}{dt} = -\frac{\partial \mathcal{H}}{\partial H_I}, \quad \frac{d\xi_3}{dt} = -\frac{\partial \mathcal{H}}{\partial V_W}, \quad \frac{d\xi_4}{dt} = -\frac{\partial \mathcal{H}}{\partial V_M}.$$

Therefore, the adjoint system evaluated at optimal controls $u_1(t), u_2(t)$ and corresponding to the model state variables H_S, H_I, V_W and V_M is given by

$$\begin{aligned} \frac{d\xi_1}{dt} &= (1 - u_1(t)) \beta V_W (\xi_1 - \xi_2) + \xi_1 \mu_S, \\ \frac{d\xi_2}{dt} &= -P_1 + \xi_2 \eta_I - \{ \xi_3 (1 - u_2(t)) + \xi_4 (1 - p u_2(t)) k \} \sigma, \\ \frac{d\xi_3}{dt} &= -P_2 + (1 - u_1(t)) \beta H_S (\xi_1 - \xi_2) + (\xi_3 + \xi_4) \delta_V, \\ \frac{d\xi_4}{dt} &= -P_3 + \xi_4 \delta_V. \end{aligned}$$

The transversality conditions, $\xi_1(t_f) = 0, \xi_2(t_f) = 0, \xi_3(t_f) = 0, \xi_4(t_f) = 0$. Now Pontryagin’s Maximum Principle (Pontryagin, 2018) states that the unconstrained optimal control $u^*(t)$ satisfies

$$\frac{\partial \mathcal{F}}{\partial u^*(t)} = 0. \tag{13}$$

So we find $\frac{\partial \mathcal{F}}{\partial u_i(t)}$, $i = 1, 2$ and solve for u_1^*, u_2^* by setting the partial derivatives of \mathcal{F} equal to zero. Thus, we have

$$\begin{aligned} \frac{\partial \mathcal{F}}{\partial u_1(t)} &= Q_1 u_1(t) + (\xi_1 - \xi_2)\beta H_S V_W = 0, \\ \frac{\partial \mathcal{F}}{\partial u_2(t)} &= Q_2 u_2(t) - (\xi_3 + kp\xi_4)\sigma H_I = 0. \end{aligned}$$

Solving these for the optimal control, we obtain

$$\begin{cases} u_1^*(t) = \frac{(\xi_2 - \xi_1)\beta H_S V_W}{Q_1}, \\ u_2^*(t) = \frac{(\xi_3 + kp\xi_4)\sigma H_I}{Q_2}. \end{cases}$$

Since the standard control is bounded, we conclude for the control u_1 :

$$u_1^*(t) = \begin{cases} 0, & \frac{(\xi_2 - \xi_1)\beta H_S V_W}{Q_1} \leq 0; \\ \frac{(\xi_2 - \xi_1)\beta H_S V_W}{Q_1}, & 0 < \frac{(\xi_2 - \xi_1)\beta H_S V_W}{Q_1} < 1; \\ 1, & \frac{(\xi_2 - \xi_1)\beta H_S V_W}{Q_1} \geq 1. \end{cases}$$

Hence the compact form of $u_1^*(t)$ is

$$u_1^*(t) = \max \left(\min \left(1, \frac{(\xi_2 - \xi_1)\beta H_S V_W}{Q_1} \right), 0 \right). \tag{14}$$

In similar way, we get the compact form of $u_2^*(t)$ in the form of

$$u_2^*(t) = \max \left(\min \left(1, \frac{(\xi_3 + kp\xi_4)\sigma H_I}{Q_2} \right), 0 \right). \tag{15}$$

Utilising equations (14) and (15) and taking the state system along with the adjoint system, and the transversality conditions, we have the following optimal system:

$$\begin{aligned} \frac{dH_S}{dt} &= \Lambda - (1 - u_1^*(t))\beta H_S V_W - \mu_S H_S, \\ \frac{dH_I}{dt} &= (1 - u_1^*(t))\beta H_S V_W - \eta_I H_I, \\ \frac{dV_W}{dt} &= (1 - u_2^*(t))\sigma H_I - \delta_V V_W, \\ \frac{dV_M}{dt} &= (1 - pu_2^*(t))k\sigma H_I - \delta_V V_M, \\ \frac{d\xi_1}{dt} &= (1 - u_1^*(t))\beta V_W (\xi_1 - \xi_2) + \xi_1 \mu_S, \\ \frac{d\xi_2}{dt} &= -P_1 + \xi_2 \eta_I - \{\xi_3(1 - u_2^*(t)) + \xi_4(1 - pu_2^*(t))k\}\sigma, \\ \frac{d\xi_3}{dt} &= -P_2 + (1 - u_1^*(t))\beta H_S (\xi_1 - \xi_2) + (\xi_3 + \xi_4)\delta_V, \\ \frac{d\xi_4}{dt} &= -P_3 + \xi_4 \delta_V, \\ \xi_i(t_f) &= 0, \quad i = 1, 2, 3, 4. \end{aligned} \tag{16}$$

□

We find that the optimal control system (16) is dependent on the state variables and their related adjoint variables. The optimal control problem (16) is exposing the fact that the control of the HCV infection requires to keep the level of healthy liver cells high and the level of infected liver cells and the viral load low by reducing the viral production and blocking the spread of infection. It is too complicated to derive the explicit analytical solutions of the optimal control system (16). As a result we avoid the complexities of analytical results, especially for real-life biological problems as it is difficult to convey predictions from these results. In this regard, we take support of numerical methods. The optimality conditions result in a two-point boundary value problem with initial conditions of state variables and terminal conditions for adjoint variables. We numerically solve this boundary value problem.

8 Numerical Simulation

In this Section, we are aimed to perform the numerical simulation of the system (1) without optimal control and the system (9) with optimal control using MATLAB and with the baseline parameter values as listed in Table 1. The parameter values are taken from different articles (Wodarz, 2005; Dahari et al., 2009; Smith and De Leenheer, 2003; Chatterjee et al., 2019; Chatterjee and Kumar, 2020). In the presence of two strains of HCV, the system is reasonably unpredictable and it is quite challenging to select the parameter values.

8.1 Simulation for System (1) Without Optimal Control

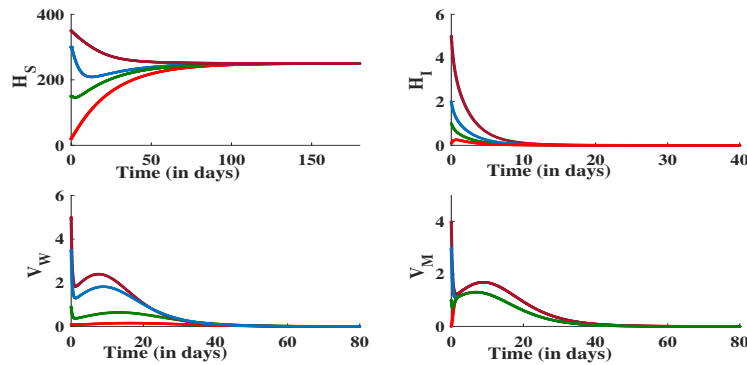


Figure 7: System trajectories with different initial conditions. The parameter values are same as put in Table 1 with $\mathcal{R}_0 = 0.832$.

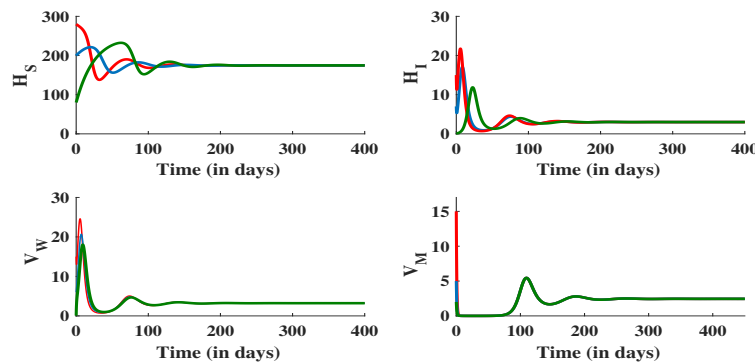


Figure 8: System trajectories with different initial conditions. The parameter values are same as put in Table 1 with $\mathcal{R}_0 = 1.536$.

We compute that the system (1) executes two equilibrium points: (i) an infection-free equilibrium $\Pi_0(250, 0, 0, 0)$ and another is (ii) the endemic equilibrium point $\Pi^*(162.699, 3.492, 4.012, 1.240)$. Using the baseline parameter values of Table 1, we calculate the basic reproduction number (\mathcal{R}_0) of the system (1) as $\mathcal{R}_0 = 0.832$.

In Figure 7, we observe that the system (1) attains the local asymptotic stability about the infection-free equilibrium point $\Pi_0(250, 0, 0, 0)$ irrespective of initial conditions for healthy liver cells (H_S), infected liver cells (H_I), wild virus strain (V_W), and

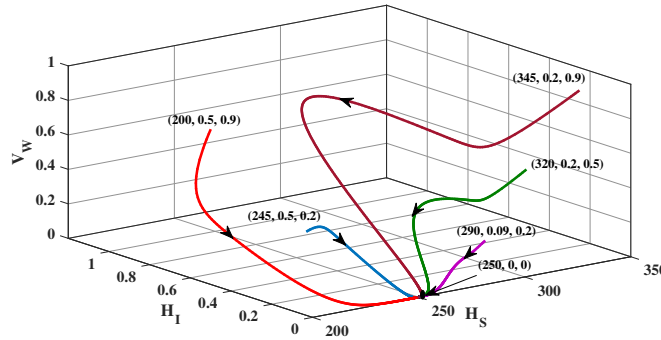


Figure 9: The phase portrait of the system (1) in the $H_S - H_I - V_W$ phase space around $\Pi_0(250, 0, 0, 0)$. The parametric values are same as listed in Table 1 with $\mathcal{R}_0 = 0.832$.

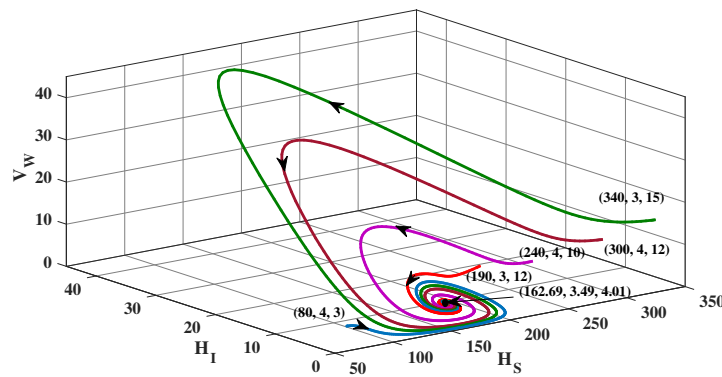


Figure 10: The phase portrait of the system (1) in the $H_S - H_I - V_W$ phase space around $\Pi^*(162.699, 3.492, 4.012, 1.240)$. The parametric values are same as listed in Table 1 with $\mathcal{R}_0 = 1.536$.

mutant virus strain (V_M) with $\mathcal{R}_0 = 0.832 < 1$. The Figure 8 indicates the existence of the endemic equilibrium and local asymptotic stability of the system (1) about the endemic equilibrium $\Pi^*(162.699, 3.492, 4.012, 1.240)$ irrespective of different initial conditions for healthy liver cells (H_S), infected liver cells (H_I), wild virus strain (V_W), and mutant virus strain (V_M) taking the removal rate of both wild virus and mutant virus $\delta_V = 1.3$; the remaining parameter values are same as put in Table 1 with $\mathcal{R}_0 = 1.536 > 1$.

The plot in Figure 9 describes that system (1) is globally asymptotically stable around the infection-free equilibrium point $\Pi_0(250, 0, 0, 0)$ in the $H_S - H_I - V_W$ phase space considering different initial conditions taking the rest of the parameters values as same as put in Table 1 with $\mathcal{R}_0 = 0.832 < 1$. The plot in Figure 10 indicates that the system (1) is globally asymptotically stable around the endemic equilibrium point $\Pi^*(162.699, 3.492, 4.012, 1.240)$ in the $H_S - H_I - V_W$ phase space considering different initial conditions and taking the removal rate of both wild and mutant virus, $\delta_V = 1.3$; the rest of the parameters values are same as put in Table 1 with $\mathcal{R}_0 = 1.536$.

8.2 Simulation for System (9) With Optimal Control

Numerical simulation to the optimal system (9) corresponding to the initial/final conditions are presented here. Our main target is to derive the control strategy for which the side effects of the antiviral drugs as well as the cost of the treatment would be minimized. Our optimal control problem is a two-point boundary value problem with boundary conditions at $t_0 = 0$ and $t_f = 500$. To solve the optimal control problem we make a change where $T = t/t_f$ and transfer the interval in $[0, 5]$, where T represents the step size with a line search method. We perform an efficiency analysis and cost-effectiveness analysis on the basis of following control strategies:

Strategy A: where $u_1(t) \neq 0, u_2(t) = 0$;

Strategy B: where $u_1(t) = 0, u_2(t) \neq 0$;

Strategy C: where $u_1(t) \neq 0, u_2(t) \neq 0$.

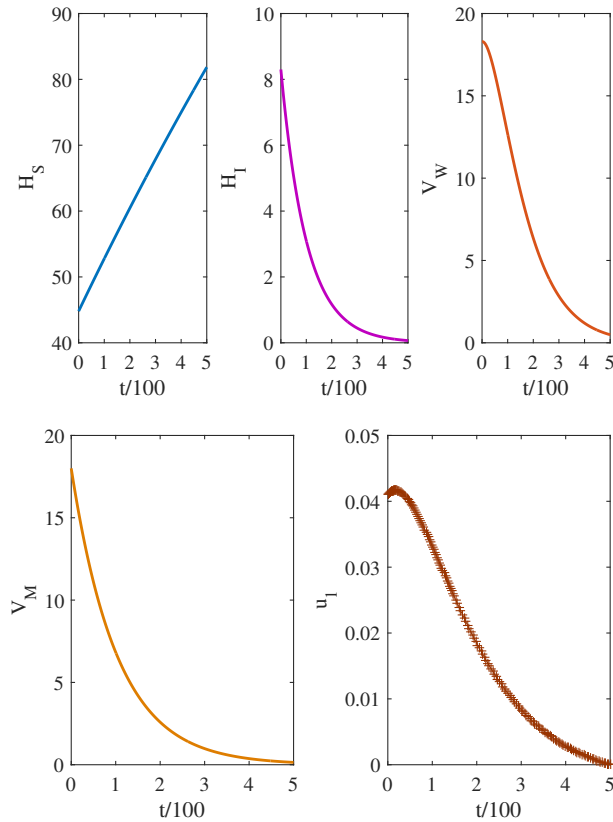


Figure 11: Strategy A: Trajectories of the control function $u_1(t)$ and of the state variables with control, keeping $Q_1 = 2$ and rest of the baseline parameter values are taken from Table 1.

Strategy A Using only $u_1(t)$ to minimize the cost function (10). In Figure 11, Strategy A shows that the healthy liver cells load increases 82.7% and infected liver cells load declines 99.2% during the treatment schedule. Also the wild type virus load declines 97.3%. This figure also shows the behaviors of the optimal control $u_1(t)$ which is employed.

Strategy B Using only $u_2(t)$ to minimize the cost function (10). In Figure 12, Strategy B shows that the healthy liver cells load increases 82.9% and infected liver cells load declines 99.3% during the treatment schedule. Also the wild type virus load declines 98.57%. The figure also describes the behaviors of the optimal control $u_2(t)$ that is employed.

Strategy C Using both $u_1(t)$ and $u_2(t)$ to minimize the cost function (10). In Figure 13, Strategy C shows that the healthy liver cells load increases 82.7% and infected liver cells load declines 99.3% during the treatment schedule. Also the wild type virus load declines 98.57%. The figure also states the behaviors of the optimal controls $u_1(t)$ and $u_2(t)$ that are employed.

8.2.1 Efficiency Analysis

Next we perform the efficacy analysis to compare the performance of the above mentioned control strategies in declining the infected liver cells load by the introduction of the efficiency index, designed by \mathcal{E} define as

$$\mathcal{E} = \left(1 - \frac{\Omega^c}{\Omega^s}\right) \times 100\%,$$

where the cumulative infected liver cells load is denoted as Ω^C when different control strategies are implemented and the cumulative infected liver cells load in absence of any control strategy is denoted as Ω^S . According to [Carvalho et al. \(2019\)](#); [Abboubakar et al. \(2018\)](#), we define the area of the cumulative infected liver cells load during the time interval $[0, T]$ is denoted by

$$\Omega = \int_0^T H_I dt.$$

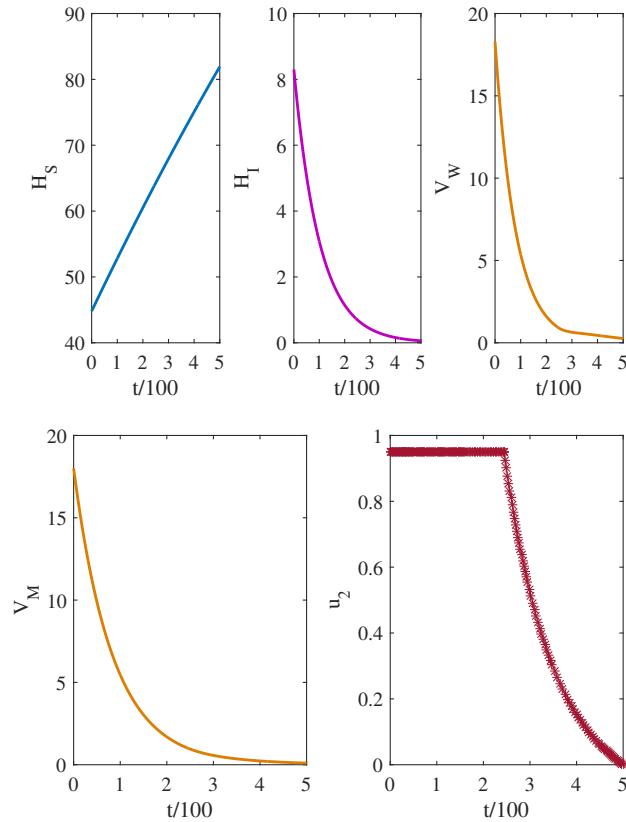


Figure 12: Strategy B: Trajectories of the control function $u_2(t)$ and of the state variables with control, keeping $Q_2 = 2$ and rest of the baseline parameter values are taken from Table 1.

Best strategy to reduce the infected cells load to decline the infection optimally can be adopted on the basis of efficiency index; the best strategy has the biggest efficiency index (Carvalho et al., 2019; Abboubakar et al., 2018). We can solve Ω numerically using Simpson's $\frac{1}{3}$ rd rule. With the help of previous simulations, we summarize the values of Ω and the efficiency index \mathcal{E} for three strategies which are listed in Table 3.

Table 3: Table of Efficiency index.

Strategy	$\Omega = \int_0^T H_I dt$	$\mathcal{E} = \left(1 - \frac{\Omega^c}{\Omega^s}\right) \times 100\%$
No Strategy	29.84	0%
A	8.4092	71.84%
B	8.3271	72.09%
C	8.3212	72.12%

From the Table 3, we can conclude that Strategy B is effective in comparison to Strategy A, but Strategy C (which is the combination of SOF and VEL) is the best strategy among these three strategies.

8.2.2 Cost-Effectiveness Analysis

Efficiency analysis benefits to determine the best strategy to decline the infected liver cells load optimally irrespective of the cost linked with each of the three control strategies. Now its an important question that among these three strategies which is of the minimum cost. After determination of the best strategy at the minimum cost, we minimize the objective functional (10) to apply the strategy in controlling the HCV infection on a large scale of population. Cost-effectiveness analysis is supported with pharmaceutical interventions or strategies in order to validate the cost of the strategies (Cantor and Ganiats, 1999; Fiscella and Franks, 1996; Pinkerton et al., 1998). We can achieve the best cost-effective strategy by comparing the differences among the

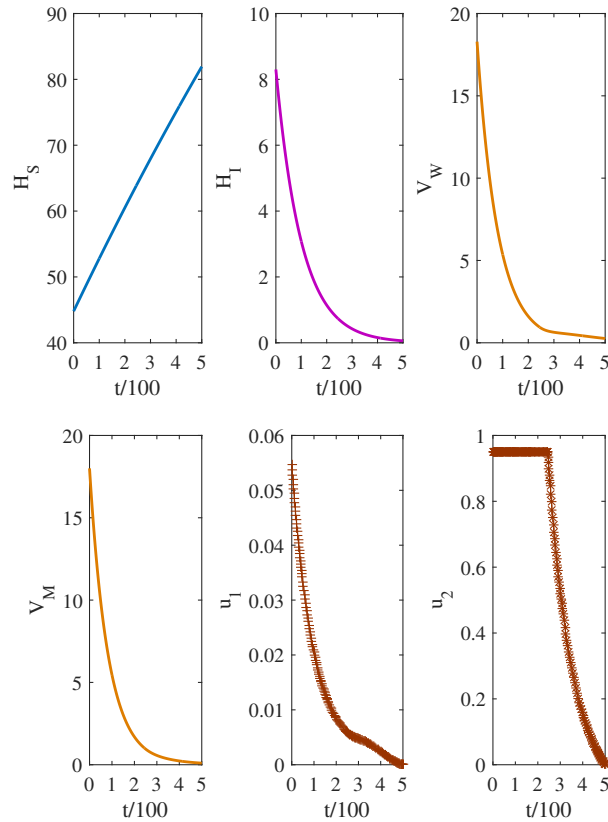


Figure 13: Strategy C: Trajectories of the control functions $u_1(t)$, $u_2(t)$ and of the state variables with control, keeping $Q_1 = Q_2 = 2$, rest of the parameter values are taken from Table 1.

costs and the health outcomes of the corresponding intervention strategies which are obtained by calculating the Incremental Cost-Effectiveness Ratio (ICER).

ICER is mainly used to determine the best between two competing control measures by comparing one intervention with the next less effective alternative (Olaniyi et al., 2020; Agosto and Adekunle, 2014). Following Agosto and Adekunle (2014), we can calculate the cost-effectiveness through ICER which is mostly defined as the additional cost per additional health outcome and to calculate ICER, we have to follow the rule

$$\text{ICER} = \frac{\text{The differences in intervention costs}}{\text{The differences in health outcomes}}.$$

The cost of each of the three control strategies is obtained from the cost functional (10) and the health outcomes (e.g. total number of infections prevented, number of susceptibility cases prevented) is measured by the difference between the load of infected liver cells without and with control (Olaniyi et al., 2020; Agosto and Adekunle, 2014). Since the cost of the control is directly proportionate to the numbers of control used, thus we rank the strategies in increasing order of effectiveness established on infection prevented based on the numerical simulations of the optimal system (9) (Agusto and Adekunle, 2014). The ascending order of the strategies is Strategy C, Strategy B, and Strategy A.

The ICER is calculated by the following technique:

$$\begin{aligned} \text{ICER}(C) &= \frac{123.4672}{8.3190} = 14.8416, \\ \text{ICER}(B) &= \frac{121.9765 - 117.87}{8.3212 - 8.3190} = 1866, \\ \text{ICER}(A) &= \frac{1.573 - 121.9765}{8.4064 - 8.3212} = -1408.45. \end{aligned}$$

Relating ICER of Strategy B and Strategy C from above calculation, a cost beneficial of 14.8416 is witnessed for Strategy C, which is above Strategy B. Thus Strategy B is more expensive and less effective than Strategy C. Hence, Strategy B is left out

from the set of options. Now Strategy B is omitted and Strategy C is then matched by Strategy A.

$$\begin{aligned} \text{ICER}(C) &= \frac{123.4672}{8.3190} = 14.8416, \\ \text{ICER}(A) &= \frac{1.573 - 123.4672}{8.4064 - 8.3190} = -1395.08. \end{aligned}$$

Now, to relate strategies ICER (A) and ICER (C) we verify that a cost beneficial of 1395.08 is witnessed for Strategy A which is above Strategy C. Negative ICER for Strategy A recommends that Strategy C is strongly dominated. Hence Strategy C is more expensive and less operative than Strategy A. Consequently, Strategy C is omitted. Therefore the above results indicate that Strategy A has the least ICER. Hence Strategy A is the most cost beneficial and effective strategy.

9 Discussion and Conclusions

We have presented a four-dimensional deterministic model to discover the kinetics of Hepatitis C virus (HCV) infection affecting the healthy liver cells. We consider two types of virus strain, viz., wild type and mutant type (with no infectivity). In treatment of HCV infection, direct-acting antivirals (DAA) have a remarkably large impact, specifically for HCV infected individuals with high rates of antiviral response. In our proposed model, we consider the effect of Sofosbuvir (SOF) and Velpatasvir (VEL) as DAA agents acting against HCV infection. Our model satisfies the non-negative initial condition (2) for a positive invariant set Ω defined in Section 3 (see Theorem 1). We derive the basic reproduction number (\mathcal{R}_0) of the system (1) around the infection-free equilibrium point $\Pi_0(\Lambda/\mu_S, 0, 0, 0)$ (see Theorem 2), such that for $\mathcal{R}_0 > 1$, the system (1) has unique positive endemic steady state. We find out that the system (1) is locally asymptotically stable around the infection-free equilibrium point $\Pi_0(\Lambda/\mu_S, 0, 0, 0)$ while $\mathcal{R}_0 < 1$ and unstable if $\mathcal{R}_0 > 1$ (see Theorem 3). Also, the system experiences a transcritical bifurcation at $\mathcal{R}_0 = 1$ (see Theorem 4). From Theorem 5, we obtain that the system (1) is locally asymptotically stable around the endemic steady state when $\mathcal{R}_0 > 1$ and unstable otherwise. We study that the global stability of the system (1) around endemic equilibrium point by constructing the suitable Lyapunov function (8). We perform sensitivity analysis to detect the effect of the model parameters on prevalence, transmission and eradication of HCV infection and we observe that the most effective parameters are $\sigma, \beta, \Lambda, \mu_s, \eta_I$ and ∂_V .

The main focus of our study is to find out the optimal strategy which comes up with minimum side effects along with minimum cost of the antiviral treatment. From that viewpoint, we use two time-dependent control functions to formulate an optimal control problem along with an objective functional in Section 7. We calculate the optimality of the system (9) in view of the mixture of SOF/VEL antiviral therapy. Analytically we verify the existence conditions and determine the necessary conditions for optimality for which the objective functional \mathcal{J} will be minimized. The analytical and numerical results (see Figure 11, Figure 12, Figure 13) highlight the effective control measures of the HCV infection by reducing the level of infected liver cells as well as decline in viral load.

We formulate the optimal control problem to restrict healthy liver cells to a high level and minimize the cost of the drugs. We observe that antiviral drug therapy has a very desirable effect upon the load of healthy liver cells. The healthy liver cells load increases to near its maximum level for almost the entire length of treatment. Simultaneously, the infection level decreases to very low level but would never be eradicated. Also at the end of the treatment schedule, when the drug level is no longer prescribed, the infection level begins to rise again. Thus we suggest that high/low or on/off drug treatment may work well to keep infection under control. This could be tested clinically via drug trials, but also mathematically using a periodic control.

Henceforth in this article, analysing our proposed deterministic model depicting the dynamical behaviors of Hepatitis C virus infection and its control both analytically and numerically, we achieve the following outcomes:

- The system attains its locally infection-free state when $\mathcal{R}_0 < 1$.
- The sensitivity analysis benefits to detect the most sensitive parameters for HCV infection and their effects in prevalence, progression and mitigation of the infection.
- The DAA treatment has a significant impact to reduce the infection level and viral load.
- The infected liver cells load can be smoothed by proper administration of control.
- With respect to efficiency, Strategy C (SOF/VEL) is ideal strategy among three strategies.
- Strategy A (use of SOF) is the best cost beneficial strategy among three strategies.

Acknowledgments

This research was supported to Piu Samui to pursue her Ph.D. (Swami Vivekananda Merit-cum-Means Scholarship) from the West Bengal Higher Education Department, Govt. of West Bengal, Bikash Bhavan, India with G. O. No. 52-Edn(B)/5B-15/2017 dated 07.06.2017.

References

- Abboubakar, H., J. C. Kamgang, L. N. Nkamba, and D. Tieudjo (2018). Bifurcation thresholds and optimal control in transmission dynamics of arboviral diseases. *Journal of Mathematical Biology* 76(1-2), 379–427. 207, 208
- Agusto, F. and A. Adekunle (2014). Optimal control of a two-strain tuberculosis-HIV/AIDS co-infection model. *Biosystems* 119, 20–44. 209
- Banerjee, S., R. Keval, and S. Gakkhar (2013). Modeling the dynamics of hepatitis C virus with combined antiviral drug therapy: Interferon and ribavirin. *Mathematical biosciences* 245(2), 235–248. 191
- Birkhoff, G. and G. C. Rota (1962). *Ordinary differential equations*. Ginn. 202
- Boyce, W. E. and R. C. DiPrima (2012). *Elementary differential equations and boundary value problems*. John Wiley & Sons, Inc. All rights reserved. 202
- Cantor, S. B. and T. G. Ganiats (1999). Incremental cost-effectiveness analysis: the optimal strategy depends on the strategy set. *Journal of clinical epidemiology* 52(6), 517–522. 208
- Carvalho, S. A., S. O. da Silva, and I. da Cunha Charret (2019). Mathematical modeling of dengue epidemic: control methods and vaccination strategies. *Theory in Biosciences* 138(2), 223–239. 207, 208
- Chakrabarty, S. P. and H. R. Joshi (2009). Optimally controlled treatment strategy using interferon and ribavirin for hepatitis C. *Journal of Biological Systems* 17(01), 97–110. 191
- Chatterjee, A. N., F. Al Basir, and Y. Takeuchi (2021). Effect of DAA therapy in hepatitis C treatment—an impulsive control approach. *Mathematical Biosciences and Engineering* 18(2), 1450–1464. 191
- Chatterjee, A. N. and B. Kumar (2020). Cytotoxic T-lymphocyte vaccination for hepatitis C: A mathematical approach. *Studies in Indian Place Names* 40(56), 769–779. 191, 205
- Chatterjee, A. N., M. K. Singh, and B. Kumar (2019). The effect of immune responses in HCV disease progression. *Eng. Math. Lett.* 2019, Article-ID. 191, 205
- Chowdhury, S., P. K. Roy, et al. (2016). Mathematical modelling of enfuvirtide and protease inhibitors as combination therapy for HIV. *International Journal of Nonlinear Sciences and Numerical Simulation* 17(6), 259–275. 198
- Dahari, H., J. E. Layden-Almer, E. Kallwitz, R. M. Ribeiro, S. J. Cotler, T. J. Layden, and A. S. Perelson (2009). A mathematical model of hepatitis C virus dynamics in patients with high baseline viral loads or advanced liver disease. *Gastroenterology* 136(4), 1402–1409. 193, 205
- Dahari, H., A. Lo, R. M. Ribeiro, and A. S. Perelson (2007). Modeling hepatitis C virus dynamics: liver regeneration and critical drug efficacy. *Journal of theoretical biology* 247(2), 371–381. 191
- Diekmann, O., J. A. P. Heesterbeek, and J. A. Metz (1990). On the definition and the computation of the basic reproduction ratio R_0 in models for infectious diseases in heterogeneous populations. *Journal of mathematical biology* 28(4), 365–382. 194
- Dixit, N. M., J. E. Layden-Almer, T. J. Layden, and A. S. Perelson (2004). Modelling how ribavirin improves interferon response rates in hepatitis C virus infection. *Nature* 432(7019), 922–924. 191
- Feld, J. J. and J. H. Hoofnagle (2005). Mechanism of action of interferon and ribavirin in treatment of hepatitis C. *Nature* 436(7053), 967–972. 191
- Fiscella, K. and P. Franks (1996). Cost-effectiveness of the transdermal nicotine patch as an adjunct to physicians' smoking cessation counseling. *Jama* 275(16), 1247–1251. 208

- Fleming, W. H. and R. W. Rishel (2012). *Deterministic and stochastic optimal control*, Volume 1. Springer Science & Business Media. 201
- Gantmacher, F. R. and J. L. Brenner (2005). *Applications of the Theory of Matrices*. Courier Corporation. 197
- Hurwitz, A. et al. (1964). On the conditions under which an equation has only roots with negative real parts. *Selected papers on mathematical trends in control theory* 65, 273–284. 197
- Korobeinikov, A. and P. K. Maini (2004). A Lyapunov function and global properties for SIR and SEIR epidemiological models with nonlinear incidence. *Mathematical Biosciences & Engineering* 1(1), 57. 197
- Lawitz, E. J., H. Dvory-Sobol, B. P. Doehle, A. S. Worth, J. McNally, D. M. Brainard, J. O. Link, M. D. Miller, and H. Mo (2016). Clinical resistance to velpatasvir (GS-5816), a novel pan-genotypic inhibitor of the hepatitis C virus NS5A protein. *Antimicrobial agents and chemotherapy* 60(9), 5368–5378. 191
- Lukes, D. L. (1982). Differential equations: classical to controlled. 201, 202
- McCluskey, C. C. (2010). Global stability for an SIR epidemic model with delay and nonlinear incidence. *Nonlinear Analysis: Real World Applications* 11(4), 3106–3109. 197
- Mogalian, E., P. German, B. P. Kearney, C. Y. Yang, D. Brainard, J. Link, J. McNally, L. Han, J. Ling, and A. Mathias (2017). Preclinical pharmacokinetics and first-in-human pharmacokinetics, safety, and tolerability of velpatasvir, a pangenotypic hepatitis C virus NS5A inhibitor, in healthy subjects. *Antimicrobial agents and chemotherapy* 61(5). 191
- Neumann, A. U., N. P. Lam, H. Dahari, D. R. Gretch, T. E. Wiley, T. J. Layden, and A. S. Perelson (1998). Hepatitis C viral dynamics in vivo and the antiviral efficacy of interferon- α therapy. *Science* 282(5386), 103–107. 191
- Olaniyi, S., O. Obabiyi, K. Okosun, A. Oladipo, and S. Adewale (2020). Mathematical modelling and optimal cost-effective control of COVID-19 transmission dynamics. *The European Physical Journal Plus* 135(11), 1–20. 209
- Perko, L. (2013). *Differential equations and dynamical systems*, Volume 7. Springer Science & Business Media. 196
- Pinkerton, S. D., D. R. Holtgrave, W. J. DiFrancesco, L. Y. Stevenson, and J. A. Kelly (1998). Cost-effectiveness of a community-level HIV risk reduction intervention. *American Journal of Public Health* 88(8), 1239–1242. 208
- Pontryagin, L. S. (2018). *Mathematical theory of optimal processes*. Routledge. 201, 203, 204
- Powers, K. A., N. M. Dixit, R. M. Ribeiro, P. Golia, A. H. Talal, and A. S. Perelson (2003). Modeling viral and drug kinetics: hepatitis C virus treatment with pegylated interferon alfa-2b. In *Seminars in liver disease*, Volume 23, pp. 013–018. Copyright© 2002 by Thieme Medical Publishers, Inc., 333 Seventh Avenue, New York. 191
- Routh, E. J. (1877). *A Treatise on the Stability of a Given State of Motion, Particularly Steady Motion: Being the Essay to which the Adams Prize was Adjudged in 1877, in the University of Cambridge*. Macmillan and Company. 197
- Samui, P., J. Mondal, and S. Khajanchi (2020). A mathematical model for COVID-19 transmission dynamics with a case study of India. *Chaos, Solitons & Fractals*, 110173. 197
- Smith, H. L. and P. De Leenheer (2003). Virus dynamics: a global analysis. *SIAM Journal on Applied Mathematics* 63(4), 1313–1327. 193, 205
- Van den Driessche, P. and J. Watmough (2002). Reproduction numbers and sub-threshold endemic equilibria for compartmental models of disease transmission. *Mathematical biosciences* 180(1-2), 29–48. 194
- Von Felden, J., J. Vermehren, P. Ingiliz, S. Mauss, T. Lutz, K. Simon, H. Busch, A. Baumgarten, K. Schewe, D. Hueppe, et al. (2018). High efficacy of sofosbuvir/velpatasvir and impact of baseline resistance-associated substitutions in hepatitis C genotype 3 infection. *Alimentary pharmacology & therapeutics* 47(9), 1288–1295. 191, 192
- Wodarz, D. (2005). Mathematical models of immune effector responses to viral infections: Virus control versus the development of pathology. *Journal of computational and applied mathematics* 184(1), 301–319. 193, 205
- World Health Organization (2020). Hepatitis C. <https://www.who.int/news-room/fact-sheets/detail/hepatitis-c>. 191

- Younossi, Z. M., M. Stepanova, J. Feld, S. Zeuzem, I. Jacobson, K. Agarwal, C. Hezode, F. Nader, L. Henry, and S. Hunt (2016). Sofosbuvir/velpatasvir improves patient-reported outcomes in HCV patients: Results from ASTRAL-1 placebo-controlled trial. *Journal of hepatology* 65(1), 33–39. [192](#)
- Younossi, Z. M., M. Stepanova, J. Feld, S. Zeuzem, M. Sulkowski, G. R. Foster, A. Mangia, M. Charlton, J. G. O’Leary, M. P. Curry, et al. (2017). Sofosbuvir and velpatasvir combination improves patient-reported outcomes for patients with HCV infection, without or with compensated or decompensated cirrhosis. *Clinical Gastroenterology and Hepatology* 15(3), 421–430. [192](#)
- Younossi, Z. M., M. Stepanova, M. Sulkowski, G. R. Foster, N. Reau, A. Mangia, K. Patel, N. Bräu, S. K. Roberts, N. Afdhal, et al. (2016). Ribavirin-free regimen with sofosbuvir and velpatasvir is associated with high efficacy and improvement of patient-reported outcomes in patients with genotypes 2 and 3 chronic hepatitis C: results from astral-2 and-3 clinical trials. *Clinical Infectious Diseases* 63(8), 1042–1048. [192](#)